A Well-Conditioned Hierarchical Basis for Triangular *H*(**curl**)-Conforming Elements

Jianguo Xin and Wei Cai*

Department of Mathematics and Statistics, University of North Carolina, Charlotte, NC 28223, USA.

To the memory of David Gottlieb

Abstract. We construct a well-conditioned hierarchical basis for triangular *H*(**curl**)-conforming elements with selected orthogonality. The basis functions are grouped into edge and interior functions, and the later is further grouped into normal and bubble functions. In our construction, the trace of the edge shape functions are orthonormal on the associated edge. The interior normal functions, which are perpendicular to an edge, and the bubble functions are both orthonormal among themselves over the reference element. The construction is made possible with classic orthogonal polynomials, viz., Legendre and Jacobi polynomials. For both the mass matrix and the quasi-stiffness matrix, better conditioning of the new basis is shown by a comparison with the basis previously proposed by Ainsworth and Coyle [Comput. Methods. Appl. Mech. Engrg., 190 (2001), 6709-6733].

1 Introduction

The Nédélec elements [17] are the natural choices when problems in electromagnetism are solved by finite element methods. Hierarchical bases are more convenient to use when a *p*-refinement technique is applied with the finite element methods [6,7]. Webb [27] constructed hierarchical vector bases of arbitrary order for triangular and tetrahedral finite elements. It was shown [11] that the basis functions in [27] indeed span the true Nédélec space [17]. A basis in terms of affine coordinates was also given [11]. Inspired by the foundational work [17] and following Webb [27], many researchers had constructed

---

*Corresponding author. *Email addresses:* `jxin@uncc.edu` (J. Xin), `wcai@uncc.edu` (W. Cai)

various hierarchical bases for several common elements in 2D and 3D [1,3–5,14,15,18,22, 25]. Meanwhile, using the perspective of differential forms, Hiptmair [12] laid a general framework for canonical construction of *H*(**curl**)- and *H*(**div**)-conforming finite elements. For further details, the reader is referred to the works [13,19–21] and the monograph [8].

One problem with hierarchical bases is the ill-conditioning of the finite element discretization matrices for the Maxwell's equations when higher-order bases are applied [2, 27,29]. For a hierarchical basis to be useful, the issue of ill-conditioning has to be resolved. Using Gram-Schmidt orthogonalization procedure, Webb [27] gave the explicit formulas of the basis functions up to third order for triangular and tetrahedral elements. Following the same line of development [27], i.e., decomposing the basis functions into rotational and irrotational groups, Sun and collaborators [25] investigated the conditioning issue more carefully and also gave the basis functions up to the third order. Ainsworth and Coyle [3] studied both the dispersive and conditioning issues for the hierarchical basis on hybrid quadrilateral/triangular meshes. With the aid of Jacobi polynomials, the interior bubble functions are orthogonal over the equilateral reference triangle [3]. With this partial orthogonality it was shown that the condition numbers of both the mass matrix and the stiffness matrix could be reduced significantly [3]. Using Legendre polynomials, Jørgensen et al. constructed a near-orthogonal basis for the quadrilaterals and indicated that the same procedure could be applied for the triangles with the help of collapsed coordinate system [16]. More recently, Schöberl and Zaglmayr [22] created bases for highorder Nédélec elements with the property of local complete sequence to partially address the ill-conditioning issue. The key component in their construction [22] is to use (i) the gradients of scalar basis functions and, (ii) scaled and integrated Legendre polynomials. However, the ill-conditioning issue was pronounced with higher-order approximation and moderate growth of the condition number was reported [22]. A new hierarchical basis with uncommon orthogonality properties was constructed by Ingelström [14] for tetrahedral meshes where higher-order basis functions vanished if they were projected onto the relatively lower-order *H*(**curl**)-conforming spaces [14]. It was shown [14] that such a basis was well suited for use with multi-level solvers. Recently, using the orthogonalization procedure by Shreshevskii [24] and conforming to the Nédélec [17] condition, Abdul-Rahman and Kasper proposed a new hierarchical basis for the tetrahedral element [1].

The Gram-Schmidt scheme used by Webb [27] or the orthogonalization method applied by Abdul-Rahman and Kasper [1] involves a linear system of equations to be solved, and the coefficients associated with the basis functions in general cannot be expressed in closed forms. The focus of the current work is to construct a well-conditioned hierarchical basis for the triangular *H*(**curl**)-conforming elements without using the Gram-Schmidt orthogonalization. This is accomplished by using integrated Legendre polynomials for higher-order edge functions and Jacobi polynomials for interior functions. The basis functions of any approximation order are given explicitly in closed form. Our work is based upon the studies by Ainsworth and Coyle [3], and by Schöberl and Zaglmayr [22], and motivated by the study of orthogonal polynomials of several variables [9].

The rest of this paper is organized as follows. In Section 2 the reference element is defined along with some preliminary results. The construction of basis functions is given in Section 3. Numerical results of matrix conditioning are shown in Section 4. Concluding remarks are presented in Section 5. For the convenience of practitioners, explicit formulas of the basis functions up to tenth order are given in the Appendix. The graphs of the shape functions up to order five are also shown in the Appendix.

2   Reference element and preliminary

We construct basis functions for the triangular *H*(**curl**)-conforming elements on a canonical reference element since any triangle can be transformed into the reference element by a linear bijective mapping. Instead of using the equilateral triangle as the reference element [3], we consider the standard 2-simplex *K* which is defined by

$$K := \left\{ (\xi, \eta) \in \mathbb{R}^2 : 0 \leq \xi, \eta; \ \xi + \eta \leq 1 \right\}. \tag{2.1}$$

The notation for the reference element is shown in Fig. 1. The coordinates for the vertexes are $V_1(1,0)$, $V_2(0,1)$ and $V_3(0,0)$. Each edge is the directed line segment which is named in terms of the opposite vertex, i.e., $\Gamma_1 := V_2 \to V_3$, $\Gamma_2 := V_3 \to V_1$, and $\Gamma_3 := V_1 \to V_2$ and their corresponding unit direction vector is denoted as $\widehat{\Gamma}_i, i = 1, 2, 3$. The barycentric coordinates of the reference element are simply

$$\lambda_1 = \xi, \quad \lambda_2 = \eta, \quad \lambda_3 = 1 - \xi - \eta. \tag{2.2}$$

In terms of the barycentric coordinates, each edge can be parametrized as

$$\tau_1|_{\Gamma_1} = \lambda_3 - \lambda_2, \quad \tau_2|_{\Gamma_2} = \lambda_1 - \lambda_3, \quad \tau_3|_{\Gamma_3} = \lambda_2 - \lambda_1. \tag{2.3}$$

The parameter varies in the range $\tau_i = [-1, 1]$, $i = 1, 2, 3$. The normal vector on each edge is

$$\vec{n}_1 = \nabla \lambda_1 = \begin{bmatrix} 1 \\ 0 \end{bmatrix}, \quad \vec{n}_2 = \nabla \lambda_2 = \begin{bmatrix} 0 \\ 1 \end{bmatrix}, \quad \vec{n}_3 = \nabla \lambda_3 = \begin{bmatrix} -1 \\ -1 \end{bmatrix}. \tag{2.4}$$

For the construction of the basis functions, we will employ a classic result in the book [26] by Szabó and Babuška. Consider the integral of the *normalized* Legendre polynomials defined by

$$p_0^i(\tau) := \sqrt{\frac{2i-1}{2}} \int_{-1}^{\tau} P_{i-1}(\sigma) d\sigma, \quad i \geq 2, \tag{2.5}$$

where $P_{i-1}(\sigma)$ is the classic Legendre polynomials of degree $i-1$. Using the symmetry and differentiation properties of the Legendre polynomials, the above integral can be readily shown to take the form

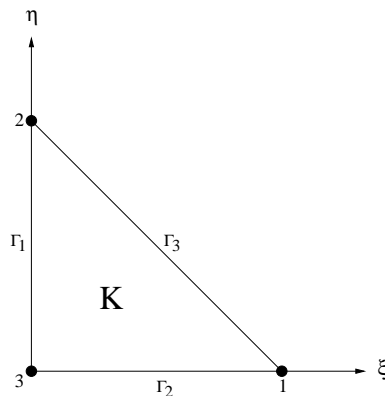$$p_0^i(\tau) = \frac{P_i(\tau) - P_{i-2}(\tau)}{\sqrt{2(2i-1)}}, \quad i \geq 2. \tag{2.6}$$

Figure 1: Canonical reference element (2-simplex).

The expression on the right-hand side, except for the scaling factor in the denominator, had been used by Jørgensen et al. [15] to construct hierarchical Legendre basis functions, and by Shen [23] to design direct solvers of second-order equations. It is clear that the newly defined polynomials have the following properties [26]:

$$p_0^i(-1) = p_0^i(1) = 0, \qquad\qquad i \geq 2, \qquad\qquad (2.7a)$$

$$\int_{-1}^{1} \frac{dp_0^{i+1}(\tau)}{d\tau} \frac{dp_0^{j+1}(\tau)}{d\tau} d\tau = \delta_{ij}, \qquad i,j \geq 1, \qquad\qquad (2.7b)$$

where δ_{ij} is the Kronecker delta function.

3 Construction of basis functions

We now construct basis functions for the **H(curl)**-conforming elements on the reference element.

3.1 Lowest-order basis

The lowest order elements are also historically called Whitney elements [28]. The basis consists of three shape functions with one on each edge, viz.,

$$\mathbf{\Phi}_{\Gamma_j}^{e,0} = |\Gamma_j|(\lambda_{j_1}\vec{n}_{j_2} - \lambda_{j_2}\vec{n}_{j_1}), \quad j=1,2,3, \qquad\qquad (3.1)$$

where

$$j_1 = \begin{cases} \mathrm{mod}(j+1,3), & \text{if } j+1 \neq 3, \\ 3, & \text{otherwise,} \end{cases} \qquad j_2 = \begin{cases} \mathrm{mod}(j+2,3), & \text{if } j+2 \neq 3, \\ 3, & \text{otherwise.} \end{cases} \qquad (3.2)$$

Written in an explicit form, these functions are

$$\mathbf{\Phi}_{\Gamma_1}^{e,0} = \lambda_2\vec{n}_3 - \lambda_3\vec{n}_2, \qquad \mathbf{\Phi}_{\Gamma_2}^{e,0} = \lambda_3\vec{n}_1 - \lambda_1\vec{n}_3, \qquad \mathbf{\Phi}_{\Gamma_3}^{e,0} = \sqrt{2}(\lambda_1\vec{n}_2 - \lambda_2\vec{n}_1). \qquad (3.3)$$

It is easy to verify that the basis functions in (3.1) has the following two important properties:

$$\nabla \cdot \mathbf{\Phi}_{\Gamma_j}^{e,0} = 0, \qquad j = 1,2,3, \tag{3.4a}$$

$$\widehat{\Gamma}_k \cdot \mathbf{\Phi}_{\Gamma_j}^{e,0} = \delta_{jk}, \quad j,k = 1,2,3. \tag{3.4b}$$

So each basis function is divergence-free, and has a constant *unit* tangential component on its associated edge and has no contribution on the other two edges.

3.2   Higher-order basis

The functions for a higher-order basis can be grouped into two classes according to their associated geometric identities on the reference element.

3.2.1   Edge-based functions

As pointed out in [22], the key idea of constructing higher-order basis functions is to incorporate the gradients of scalar functions. Schöberl and Zaglmayr [22] exploited the *scaled* integrated Legendre polynomials to construct edge-based functions. It can be shown that the shape functions on each edge are not pairwise orthogonal [22]. We construct edge-based orthonormal shape functions using the normalized but not scaled Legendre polynomials defined in (2.5). The higher-order edge-based functions are given by

$$\mathbf{\Phi}_{\Gamma_j}^{e,i-1} = \nabla \left(\frac{1}{|\nabla \tau_j|} p_0^i(\tau_j) \right), \qquad i = 2,3,\cdots,p+1, \quad j = 1,2,3, \tag{3.5}$$

where for each edge, the scaling constant is

$$|\nabla \tau_1| = \sqrt{5}, \qquad |\nabla \tau_2| = \sqrt{5}, \qquad |\nabla \tau_3| = \sqrt{2}. \tag{3.6}$$

The higher-order basis functions in (3.5) are curl-free, whose trace on the edge are orthonormal on each associated edge, viz.,

$$\nabla \times \mathbf{\Phi}_{\Gamma_j}^{e,i-1} = 0, \qquad\qquad i = 2,3,\cdots,p+1, \qquad j = 1,2,3, \tag{3.7a}$$

$$< \mathbf{\Phi}_{\Gamma_j}^{e,i-1}, \mathbf{\Phi}_{\Gamma_j}^{e,k-1} > |_{\Gamma_j} = \delta_{ik}, \qquad i,k = 2,3,\cdots,p+1, \quad j = 1,2,3, \tag{3.7b}$$

where the notation $< \bullet, \bullet >$ represents the standard inner product. The curl-free property in (3.7a) is true since each shape function is expressed in terms of a gradient. The orthonormal property in (3.7b) can be proved by noticing that the shape function can be written in the following form:

$$\mathbf{\Phi}_{\Gamma_j}^{e,i-1} = \sqrt{\frac{2i-1}{2}} \frac{\nabla \tau_j}{|\nabla \tau_j|} P_{i-1}(\tau_j), \qquad i = 2,3,\cdots,p+1, \quad j = 1,2,3, \tag{3.8}$$

and the orthogonality relation of the Legendre polynomials, viz.,

$$\int_{-1}^{1} P_i(\sigma) P_j(\sigma) d\sigma = \frac{2}{2i+1} \delta_{ij}, \qquad i,j = 0,1,2,\cdots. \tag{3.9}$$

3.2.2   Interior functions

For complete polynomial approximation of the Nédélec space with degree $p \geq 2$, interior functions are needed. Following the construction of shape functions by Webb [27] and by Ainsworth and Coyle [3], we classify the interior functions into two groups-*normal* functions and *bubble* functions. All interior functions have no tangential contribution along any edge. However, the normal functions will have normal components on their associated edges while the bubble functions are free of normal components on all edges.

Normal functions

Ainsworth and Coyle [3] constructed the interior normal functions by applying Legendre polynomials. It can be shown that the normal functions which are perpendicular to an edge are not pairwise orthogonal on the reference element [3]. By using Jacobi polynomials, we construct interior normal functions which are orthonormal on the reference element (2-simplex). The interior normal functions are given by

$$\mathbf{\Phi}_{\Gamma_j}^{n,k+2} = 8\sqrt{k+3}(1-\lambda_j)^k p_k^{(2,2)}\left(\frac{\tau_j}{1-\lambda_j}\right)\lambda_{j_1}\lambda_{j_2}\frac{\vec{n}_j}{|\vec{n}_j|}, \quad k=0,1,2,\cdots,p-2, \tag{3.10}$$

where $p_k^{(2,2)}(\bullet)$ is the orthonormal Jacobi polynomial of degree k. The subscripts j_1 and j_2 are defined in (3.2), and the scaling constant $|\vec{n}_j|$ for each edge is

$$|\vec{n}_1|=1, \qquad |\vec{n}_2|=1, \qquad |\vec{n}_3|=\sqrt{2}. \tag{3.11}$$

The interior normal functions (3.10) have two important properties, viz.,

$$\widehat{\Gamma}_j \cdot \mathbf{\Phi}_{\Gamma_i}^{n,k+2} = 0, \qquad\qquad i,j=1,2,3, \quad k=0,1,2,\cdots,p-2, \tag{3.12a}$$

$$<\mathbf{\Phi}_{\Gamma_j}^{n,i+2},\mathbf{\Phi}_{\Gamma_j}^{n,k+2}>|_K = \delta_{ik}, \quad j=1,2,3, \qquad i,k=0,1,2,\cdots,p-2. \tag{3.12b}$$

The property (3.12a), i.e., free of tangential component, can be readily seen as the normal functions (3.11) vanish on two edges and are perpendicular to the third one. The orthonormal property (3.12b) can be proved directly by using Proposition 2.3.8 in the monograph by Dunkl and Xu [9].

Bubble functions

A set of orthogonal but not *normalized* bubble functions were constructed by Ainsworth and Coyle [3]. The significant issue of scaling or normalization in constructing shape functions has already been brought to attention by Jørgensen and collaborators [15]. We construct *orthonormal* bubble functions on the reference element. Our work is motivated by the study of orthogonal polynomials of several variables [9]. First, we introduce a lemma on orthogonal polynomials over an n-simplex K [9].

Lemma 3.1. *Define polynomials on an n-simplex K*

$$P_{\vec{\alpha}}\left(W_{\vec{\kappa}}^{(K)}; \mathbf{x}\right) = \left[h_{\vec{\alpha}}^{(K)}\right]^{-1} \prod_{i=1}^{n} \left(\frac{1-|\mathbf{x}_i|}{1-|\mathbf{x}_{i-1}|}\right)^{|\vec{\alpha}^{i+1}|} p_{\alpha_i}^{(\rho_i^1, \rho_i^2)}\left(\frac{2x_i}{1-|\mathbf{x}_{i-1}|} - 1\right), \tag{3.13}$$

where $p_{\alpha_i}^{(\rho_i^1, \rho_i^2)}$ is the classic orthonormal Jacobi polynomials of one variable, $\rho_i^1 = 2|\vec{\alpha}^{i+1}| + |\vec{\kappa}^{i+1}| + (n-i-1)/2$ and $\rho_i^2 = \kappa_i - 1/2$, then, $P_{\vec{\alpha}}\left(W_{\vec{\kappa}}^{(K)}; \mathbf{x}\right)$ are orthonormal under the weight function

$$W_{\vec{\kappa}}^{(K)}(\mathbf{x}) = (1-|\mathbf{x}|)^{\kappa_{n+1}-\frac{1}{2}} \prod_{i=1}^{n} x_i^{\kappa_i - \frac{1}{2}}, \quad \mathbf{x} \in K, \quad \kappa_i \geq -\frac{1}{2}, \quad i = 1, 2, \cdots, n+1, \tag{3.14}$$

with a normalization constant $h_{\vec{\alpha}}^{(K)}$

$$\left[h_{\vec{\alpha}}^{(K)}\right]^{-2} = \prod_{i=1}^{n} 2^{\rho_i^1 + \rho_i^2 + 1}. \tag{3.15}$$

The proof of the lemma can be found in [9]. However, the normalization constant $h_{\vec{\alpha}}^{(K)}$ given in [9] is incorrect. The original normalization constant [9] has been corrected here (3.15). Using the result in Lemma 3.1, the orthonormal bubble functions can be constructed directly

$$\Phi_{i,j}^{b,p} = \{\vec{e}_\xi, \vec{e}_\eta\} \otimes h_{i,j}^K \lambda_1 \lambda_2 \lambda_3 (1-\lambda_1)^i p_i^{(2,2)}\left(\frac{\lambda_2 - \lambda_3}{1-\lambda_1}\right) p_j^{(2i+5,2)}(2\lambda_1 - 1), \tag{3.16a}$$

where

$$h_{i,j}^K = 2^{i+\frac{13}{2}}, \quad 0 \leq i, j, \, i+j \leq p-3. \tag{3.16b}$$

In our construction, we have used $\kappa_i = 5/2$, $i = 1, 2, 3$ so that the weight function is

$$W_{\vec{\kappa}}^{(K)} = (\lambda_1 \lambda_2 \lambda_3)^2. \tag{3.17}$$

The exponent in (3.16b) is obtained by the fact

$$\rho_1^1 = 2i + 5, \quad \rho_1^2 = 2, \quad \rho_2^1 = 2, \quad \rho_2^2 = 2, \quad 0 \leq i \leq p-3. \tag{3.18}$$

The interior bubble functions have the following two properties, viz.,

$$\Phi_{i,j}^{b,p}|_{\partial K} = 0, \quad 0 \leq i, j, i+j \leq p-3, \tag{3.19a}$$

$$<\Phi_{i,j}^{b,p}, \Phi_{k,\ell}^{b,q}>|_K = \delta_{ik}\delta_{j\ell}, \quad 0 \leq i, j, k, \ell, i+j \leq p-3, \, k+\ell \leq q-3. \tag{3.19b}$$

The first property (3.19a), which states that the bubble functions have vanishing tangential and normal components on the boundary (three edges) of the reference element, can be seen by noticing that the factor $\lambda_1 \lambda_2 \lambda_3$ is included with each shape function in (3.16a). The orthonormal property (3.19b) can be proved by using the result in Lemma 3.1, and by identifying $\lambda_1 = x_1$, $\lambda_2 = x_2$ and $\lambda_3 = 1 - x_1 - x_2$.

Following the same argument by Ainsworth and Coyle [3], it can be shown that the newly-constructed basis is a hierarchical basis for triangular *H*(**curl**)-conforming elements.

4 Conditioning of matrices

As in [3], we check the conditioning of the mass M and quasi-stiffness S matrices on the reference element. The components of each matrix are defined as

$$M_{i,j} := <\Phi_i, \Phi_j>|_K, \quad S_{i,j} := <\nabla \times \Phi_i, \nabla \times \Phi_j>|_K. \tag{4.1}$$

The mass matrix M is real, symmetric and positive definite, and thus its eigenvalues are all positive. The quasi-stiffness matrix S is real, symmetric and semi-positive definite, and therefore has non-negative eigenvalues.

4.1 Structure of matrices

The sparsity of the mass and quasi-stiffness matrices are shown in Table 1 and Table 2, respectively, where the shape functions for a complete polynomial approximation of order p are grouped according to their associated geometric identities.

Table 1: Sparsity of the mass matrix.

$<\bullet, \bullet>|_K$	$\Phi^e_{[3(p+1)]}$	$\Phi^n_{[3(p-1)]}$	$\Phi^b_{[(p-1)(p-2)]}$
$\Phi^e_{[3(p+1)]}$	dense	dense	sparse
$\Phi^n_{[3(p-1)]}$	dense	sparse	sparse
$\Phi^b_{[(p-1)(p-2)]}$	sparse	sparse	identity

Table 2: Sparsity of the quasi-stiffness matrix.

$<\nabla \times, \nabla \times>|_K$	$\Phi^e_{[3(p+1)]}$	$\Phi^n_{[3(p-1)]}$	$\Phi^b_{[(p-1)(p-2)]}$
$\Phi^e_{[3(p+1)]}$	sparse	O	O
$\Phi^n_{[3(p-1)]}$	O	dense	dense
$\Phi^b_{[(p-1)(p-2)]}$	O	dense	dense

To further appreciate the structure of the mass and quasi-stiffness matrices, we plot the sparsity profiles of both matrices for the approximation order $p=4$ and $p=8$ in Fig. 2 and Fig. 3, respectively.

The structure of both the mass and quasi-stiffness matrices are organized in a hierarchical way in the sense that a particular submatrix from a relatively higher-order of approximation is the matrix for a relatively lower-order of approximation. For instance, for the approximation order $p=8$, the mass matrix $M^{[p=8]}$ is a 90×90 matrix. The upper left submatrix $M^{[p=8]}_{30 \times 30}$ is the mass matrix $M^{[p=4]}$ for order $p=4$. For the mass matrices shown in Fig. 2 and with the order of approximation $p=4$, the number of nonzero entries is 618 out of 900, which is 68.67% of the entire matrix $M^{[p=4]}$. Similarly, for order $p=8$, the number of nonzero entries is 4,128 out of 8,100, which is 50.96% of the entire matrix $M^{[p=8]}$. As the order of approximation p increases, the sparsity of the mass matrix will
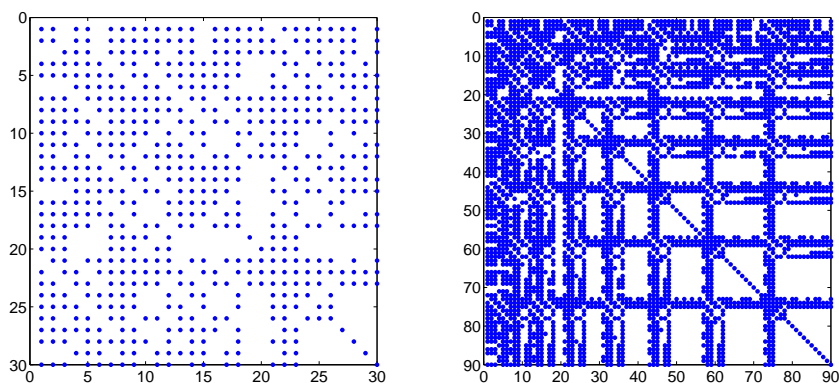
Figure 2: Structure of the mass matrices for the approximation order $p=4$ (left) and $p=8$ (right).
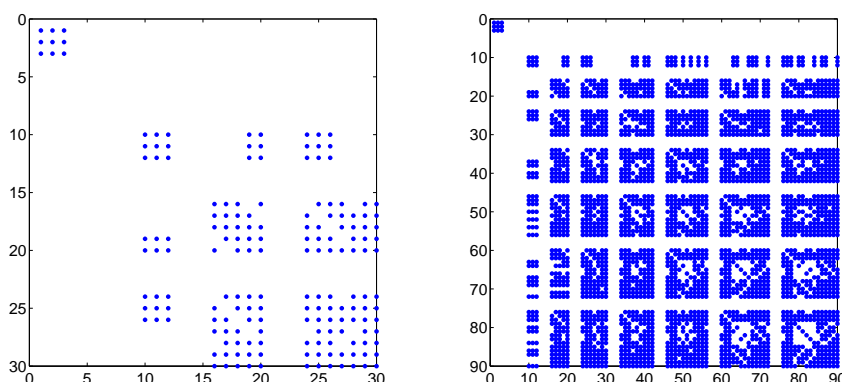

Figure 3: Structure of the quasi-stiffness matrices for the approximation order $p=4$ (left) and $p=8$ (right).

increase accordingly. The sparsity pattern of the quasi-stiffness matrix with respect to the approximation order is just opposite to that for the mass matrix. In particular, for the quasi-stiffness matrices shown in Fig. 3 and with the order of approximation $p=4$, the number of nonzero entries is 174 out of 900, which is 19.33% of the entire matrix $S^{[p=4]}$. And for order $p=8$, the number of nonzero entries is 3,146 out of 8,100, which is 38.84% of the entire matrix $S^{[p=8]}$. It should be pointed out the distinction between the sparsity and conditioning of a matrix. In general a sparse matrix does not necessarily mean that the matrix is well conditioned. Conversely, a well conditioned matrix may not be sparse. Nevertheless, a sparse matrix does have the advantage of relatively lower requirement of computer storage.

4.2 Condition numbers of mass and quasi-stiffness matrices

The condition number of a matrix A is calculated by the formula

$$\kappa(A) = \frac{\lambda^{\max}}{\lambda_{\min}}, \tag{4.2}$$

where $\lambda^{\max}$ and $\lambda_{\min}$ are the maximum and minimum eigenvalues of the matrix A, respectively. For the quasi-stiffness matrix S, only positive eigenvalues are considered. Ainsworth and Coyle [3] also considered the diagonally *normalized* mass and quasi-stiffness matrices, viz.,

$$\widetilde{M} = \Lambda_M^{-\frac{1}{2}} M \Lambda_M^{-\frac{1}{2}}, \qquad \widetilde{S} = \Lambda_S^{-\frac{1}{2}} S \Lambda_S^{-\frac{1}{2}}, \tag{4.3}$$

where Λ_M and Λ_S are the diagonal matrices of the mass M and quasi-stiffness matrices S, respectively. The condition numbers of the original and normalized mass and quasi-stiffness matrices are shown in Table 3 and Table 4, respectively. As a comparison, the condition numbers generated with the basis by Ainsworth and Coyle [3] are recorded. The ratios of the condition numbers between the A-C basis [3] and the new basis are shown in each table as well.

Table 3: Condition numbers of the mass matrix M and quasi-stiffness matrix S from the new basis and the basis in [3], denoted "A-C".

Order p	Mass		Quasi-stiffness		Ratio of two bases	
	New	A-C	New	A-C	Mass	Q.-S.
0	3.000e0	2.000e0	1.000e0	1.000e0	0.667e0	1.000e0
1	1.004e1	8.606e0	1.000e0	1.000e0	0.857e0	1.000e0
2	1.505e2	2.712e3	2.813e0	9.600e1	1.802e1	3.413e1
3	5.378e2	4.921e4	9.546e0	1.080e3	9.150e1	1.131e2
4	1.086e3	1.604e5	2.452e1	1.503e3	1.477e2	6.130e1
5	1.642e3	3.898e5	4.984e1	1.608e3	2.374e2	3.226e1
6	2.868e3	7.069e5	8.900e1	1.853e3	2.465e2	2.082e1
7	3.852e3	1.505e6	1.472e2	2.226e3	3.907e2	1.512e1
8	5.627e3	3.497e6	2.224e2	2.953e3	6.215e2	1.328e1
9	7.580e3	6.830e6	3.452e2	3.534e3	9.011e2	1.024e1
10	9.928e3	1.213e7	4.948e2	4.467e3	1.222e3	9.028e0
11	1.127e4	2.181e7	7.033e2	5.291e3	1.935e3	7.523e0
12	1.478e4	4.099e7	9.650e2	6.507e3	2.773e3	6.743e0

From Table 3 several observations on the conditioning for the original un-normalized matrices can be made.

• For the mass matrix M, starting from order 4, the conditioning with the basis in this study is at least two orders better than the basis by Ainsworth and Coyle [3]. The higher the order of approximation, the better the conditioning of the new basis. Indeed, starting from order 10, the conditioning with the new basis is at least three orders better relative to the one in [3]. For the relatively low orders, $p=2$ and $p=3$, the conditioning with the new basis is still at least one order better.

• For the quasi-stiffness matrix S, starting from order 2, the conditioning with the basis in this study is about one order better than the basis by Ainsworth and Coyle [3] though the advantage decreases as the order p increases.

Table 4: Condition numbers of the normalized mass matrix $\widetilde{M}$ and quasi-stiffness matrix $\widetilde{S}$ from the new basis and the basis in [3], denoted "A-C".

Order p	Mass		Quasi-stiffness		Ratio of two bases	
	New	A-C	New	A-C	Mass	Q.-S.
0	3.000e0	2.000e0	1.000e0	1.000e0	0.667e0	1.000e0
1	5.161e0	6.491e0	1.000e0	1.000e0	1.258e0	1.000e0
2	7.409e1	9.267e1	2.000e0	3.824e0	1.251e0	1.912e0
3	2.053e2	3.840e2	3.119e0	4.821e0	1.870e0	1.546e0
4	5.202e2	1.721e3	7.777e0	8.865e0	3.308e0	1.140e0
5	8.890e2	3.364e3	8.409e0	9.773e0	3.784e0	1.162e0
6	1.259e3	1.090e4	1.137e1	1.242e1	8.658e0	1.091e0
7	2.113e3	2.011e4	1.335e1	1.563e1	9.517e0	1.171e0
8	3.109e3	5.893e4	1.599e1	1.681e1	1.895e1	1.051e0
9	3.756e3	1.042e5	1.864e1	1.952e1	2.774e1	1.047e0
10	5.408e3	2.883e5	2.146e1	1.999e1	5.331e1	0.932e0
11	6.730e3	4.920e5	2.437e1	2.150e1	7.310e1	0.880e0
12	8.189e3	1.409e6	2.743e1	2.200e1	1.721e2	0.802e0

• For both bases, the conditioning of the mass matrix is severe and more pronounced than the quasi-stiffness matrix.

Similarly, by examining the values in Table 4 and by comparing the values in both tables, one can make a couple of remarks.

• For the normalized mass matrix $\widetilde{M}$, starting from order 1, the conditioning with the new basis is better than the one in [3]. Starting from order 8, the new basis is at least one order better relative to the one in [3], and starting from order 12, the basis in this study has begun to show two orders better conditioning than the Ainsworth-Coyle basis [3]. The higher the order of approximation, the greater the advantage with the new basis. Nevertheless, compared with the case with the original un-normalized matrix, the advantage with the normalized matrix has been reduced somewhat.

• For the normalized quasi-stiffness matrix $\widetilde{S}$ and for both bases, the conditioning is not a problem. For all orders of approximation, the condition number is on the same level and roughly the same with the two bases.

In order to see the trend of the growth with the condition numbers for both matrices, we plot the condition numbers vs. the order of approximation on a logarithmic scale. The results are shown in Fig. 4 and Fig. 5 for the mass and quasi-stiffness matrices, respectively.

From Fig. 4 one can see that for the new basis, starting from order 3, the condition number grows linearly vs. order of approximation for both the original and normalized mass matrices. For the basis in [3], starting from order 6, the condition number of the original mass matrix grows linearly vs. order of approximation; while for the normalized mass matrix, starting from order 4, the condition number increases at least *super*-linearly
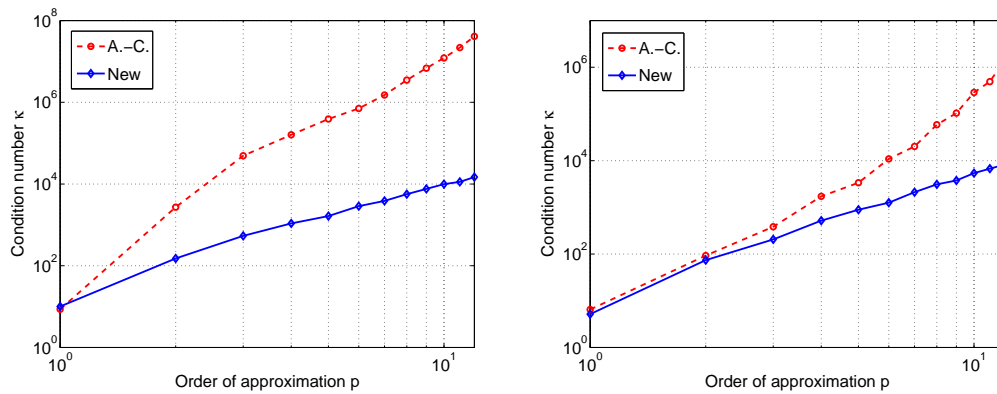
Figure 4: Condition numbers of the mass matrices: original (left) and normalized (right).
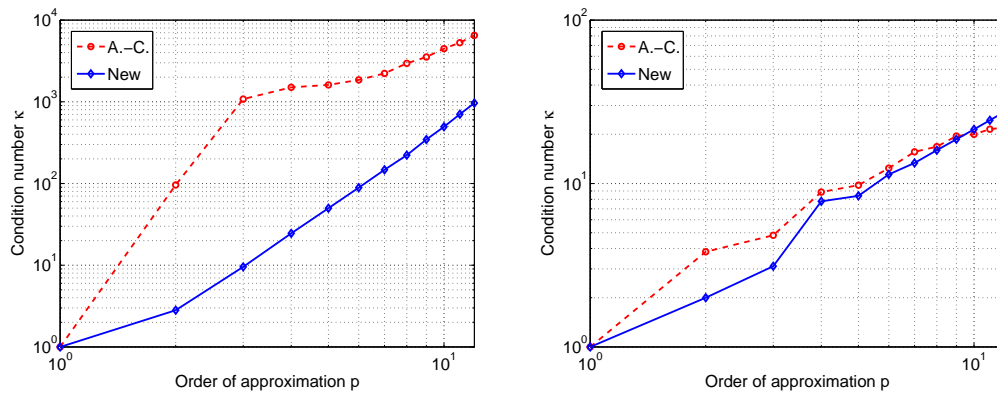

Figure 5: Condition numbers of the quasi-stiffness matrices: original (left) and normalized (right).

vs. order of approximation. Further, for both the original and normalized mass matrices, the slope of the line, i.e., the growth rate of the condition number is much higher for the basis by Ainsworth and Coyle [3]. The theoretical results [4] on the condition numbers cannot be applied to this study since they are intended for the quadrilateral and hexahedral elements.

From Fig. 5 one can identify that for the original un-normalized quasi-stiffness matrix, starting from order 2 the condition number increases linearly vs. the order of approximation for the basis in this study; and starting from order 7, the same observation holds for the Ainsworth-Coyle basis [3]. However, for the normalized quasi-stiffness matrix and for both bases, the condition numbers grow much more slowly than their corresponding un-normalized ones, and the two curves are quite close to each other. Also one can see that for the normalized quasi-stiffness matrix, there is a sudden mild jump of the condition number for the forth-order approximation with both bases. Again, the growth rates of the condition numbers for the quasi-stiffness matrices shown in Fig. 5 do not conform to the theoretical study [4], which is understandable.

4.3   Condition numbers of Schur complements

Because the Schur complement [10] plays a distinctive role in many areas, e.g., matrix and numerical analysis, we now consider for a certain approximation order p the conditioning of the Schur complements of the lower right block of the mass matrices.

We first consider the case for the approximation order $p=4$. The mass matrix can be partitioned into four (4) blocks

$$M^{[p=4]} := \begin{bmatrix} M_{11} & M_{12} \\ M_{21} & M_{22} \end{bmatrix}. \tag{4.4}$$

The submatrix M_{11} corresponds to the mass matrix $M^{[p=3]}$ for the approximation order $p=3$, i.e., $M^{[p=3]} = M_{11}$. The reason why such a partition is made is clear-due to the hierarchical structure of the mass matrix. The Schur complement of the block M_{22} is

$$M_{11}^S = M_{11} - M_{12} M_{22}^{-1} M_{21}. \tag{4.5}$$

The submatrix M_{22} is invertible since the components of this matrix are assembled from the interactions of the linearly *independent* shape functions. The condition number of the Schur complement M_{11}^S is computed and recorded as

$$\kappa(M_{11}^S) = 8.772 \times 10^2. \tag{4.6}$$

Repeat the same procedure for the diagonally normalized mass matrix $\widetilde{M}^{[p=4]}$, and it is found that

$$\kappa(\widetilde{M}_{11}^S) = 3.880 \times 10^2. \tag{4.7}$$

It is interesting to compare these two numbers with the corresponding ones in Tables 3 and 4 for the approximation order $p=3$ and $p=4$, viz.,

$$\kappa(M^{[p=3]})(5.378 \times 10^2) < \kappa(M_{11}^S)(8.772 \times 10^2) < \kappa(M^{[p=4]})(1.086 \times 10^3), \tag{4.8a}$$

$$\kappa(\widetilde{M}^{[p=3]})(2.053 \times 10^2) < \kappa(\widetilde{M}_{11}^S)(3.880 \times 10^2) < \kappa(\widetilde{M}^{[p=4]})(5.202 \times 10^2). \tag{4.8b}$$

The strict inequalities in (4.8) are understandable. From the data in (4.8) and if the technique of Schur complement [10] can be used to solve the linear system for the mass matrices, one can see that the linear system for the case with $p=4$ is relatively a little bit "harder" to solve than the case for $p=3$.

Next, for the case with the approximation order $p=8$, one can compute the Schur complements of the lower right blocks for the mass matrix $M^{[p=8]}$ and the diagonally normalized one $\widetilde{M}^{[p=8]}$. In a same manner as the case for the approximation order $p=4$, the comparison of the condition numbers of the Schur complements with the corresponding ones for the approximation order $p=7$ and $p=8$ can be made and recorded as

$$\kappa(M^{[p=7]})(3.852 \times 10^3) < \kappa(M_{11}^S)(5.518 \times 10^3) < \kappa(M^{[p=8]})(5.627 \times 10^3), \tag{4.9a}$$

$$\kappa(\widetilde{M}^{[p=7]})(2.113 \times 10^3) < \kappa(\widetilde{M}_{11}^S)(3.040 \times 10^3) < \kappa(\widetilde{M}^{[p=8]})(3.109 \times 10^3). \tag{4.9b}$$

Similarly as the case for $p\!=\!4$, the same observation can be made for the case $p\!=\!8$. The linear system for the case with $p\!=\!8$ is somehow a little bit "harder" to solve than the case for $p\!=\!7$ if the Schur complement can be used for the linear system of the mass matrices.

5 Discussion and conclusions

A new set of hierarchical basis for triangular **H**(**curl**)-conforming elements has been proposed with the goal of improving the conditioning of the mass and quasi-stiffness matrices. The basis functions are given explicitly by four formulas, viz., (3.1), (3.5), (3.10), and (3.16). The construction of the new basis is motivated by the study of orthogonal polynomials of several variables [9], and based on the work by Ainsworth and Coyle [3], and by Schöberl and Zaglmayr [22], thus combines the advantage of both works. The idea is to make each set of shape functions, grouped and associated with a geometric identity, orthonormal with respect to that particular identity on the reference 2-simplex element. This is achieved by appropriately exploiting classic orthogonal polynomials, viz., Legendre and Jacobi polynomials over simplicial elements.

The sparsity structure of the mass and quasi-stiffness matrices has been identified for two typical approximation orders. The conditioning of the Schur complements for the mass matrices has been numerically studied, and it is found that for two consecutive orders of approximation, the linear system from the relatively higher-order approximation is slightly hard to solve.

Numerical studies have shown that the conditioning of the mass matrix is relatively more salient than that with the quasi-stiffness matrix. In particular, the diagonally normalized quasi-stiffness matrix is well conditioned. For the *original un-normalized* mass matrix, in terms of matrix conditioning and starting from order four (4) of approximation, the basis in this study is at least two orders better in conditioning number than the basis proposed by Ainsworth and Coyle [3]; and starting from order ten (10), the new basis shows even greater advantage of at least three orders better. Similarly, for the diagonally *normalized* mass matrix, starting from order eight (8) of approximation, the basis in this study is at least one order better than the one by Ainsworth and Coyle [3]; and starting from order twelve (12), the proposed basis shows at least two orders better. The higher the order of approximation, the greater the advantage of the new basis, fulfilling the goal of a hierarchical basis.

Acknowledgments

Appendix

Explicit formulas of the basis functions

Up to order ten (10) of approximation and in terms of the coordinates (ξ,η) for the reference element, the formulas for the shape functions in the basis are given as follows. Some formulas are quite long, and for such cases we use short-hand notations, i.e.,

$$\star := 1-\xi-2\eta, \quad *:=2\xi+\eta-1, \quad \diamond:=2\xi-1, \quad \dagger:=\eta-\xi, \quad \wr:=1-\xi-\eta,$$

$$\natural:=1-\xi, \qquad \sharp:=1-\eta, \qquad \flat:=\xi+\eta, \qquad \bowtie:=\left\{\begin{bmatrix} 1 \\ 0 \end{bmatrix},\begin{bmatrix} 0 \\ 1 \end{bmatrix}\right\}.$$

The shape functions up to the fifth-order of approximation are shown in the following figures.

Zeroth-order

$$\Phi_{\Gamma_1}^{e,0}=\begin{bmatrix} -\eta \\ -1+\xi \end{bmatrix}, \qquad \Phi_{\Gamma_2}^{e,0}=\begin{bmatrix} 1-\eta \\ \xi \end{bmatrix}, \qquad \Phi_{\Gamma_3}^{e,0}=\sqrt{2}\begin{bmatrix} -\eta \\ \xi \end{bmatrix}.$$

First-order

$$\Phi_{\Gamma_1}^{e,1}=-\sqrt{\frac{3}{10}}(1-\xi-2\eta)\begin{bmatrix} 1 \\ 2 \end{bmatrix}, \quad \Phi_{\Gamma_2}^{e,1}=\sqrt{\frac{3}{10}}(2\xi+\eta-1)\begin{bmatrix} 2 \\ 1 \end{bmatrix}, \quad \Phi_{\Gamma_3}^{e,1}=\frac{\sqrt{3}}{2}(\eta-\xi)\begin{bmatrix} -1 \\ 1 \end{bmatrix}.$$

Second-order

$$\Phi_{\Gamma_1}^{e,2}=-\frac{\sqrt{2}}{4}\left[3(1-\xi-2\eta)^2-1\right]\begin{bmatrix} 1 \\ 2 \end{bmatrix}, \qquad \Phi_{\Gamma_2}^{e,2}=\frac{\sqrt{2}}{4}\left[3(2\xi+\eta-1)^2-1\right]\begin{bmatrix} 2 \\ 1 \end{bmatrix},$$

$$\Phi_{\Gamma_3}^{e,2}=\frac{\sqrt{5}}{4}\left[3(\eta-\xi)^2-1\right]\begin{bmatrix} -1 \\ 1 \end{bmatrix}, \qquad \Phi_{\Gamma_1}^{n,2}=6\sqrt{5}\eta(1-\xi-\eta)\begin{bmatrix} 1 \\ 0 \end{bmatrix},$$

$$\Phi_{\Gamma_2}^{n,2}=6\sqrt{5}\xi(1-\xi-\eta)\begin{bmatrix} 0 \\ 1 \end{bmatrix}, \qquad \Phi_{\Gamma_3}^{n,2}=-3\sqrt{10}\xi\eta\begin{bmatrix} 1 \\ 1 \end{bmatrix}.$$

Third-order

$$\Phi_{\Gamma_1}^{e,3}=-\frac{\sqrt{70}}{20}\left[5(1-\xi-2\eta)^3-3(1-\xi-2\eta)\right]\begin{bmatrix} 1 \\ 2 \end{bmatrix},$$

$$\Phi_{\Gamma_2}^{e,3}=\frac{\sqrt{70}}{20}\left[5(2\xi+\eta-1)^3-3(2\xi+\eta-1)\right]\begin{bmatrix} 2 \\ 1 \end{bmatrix},$$
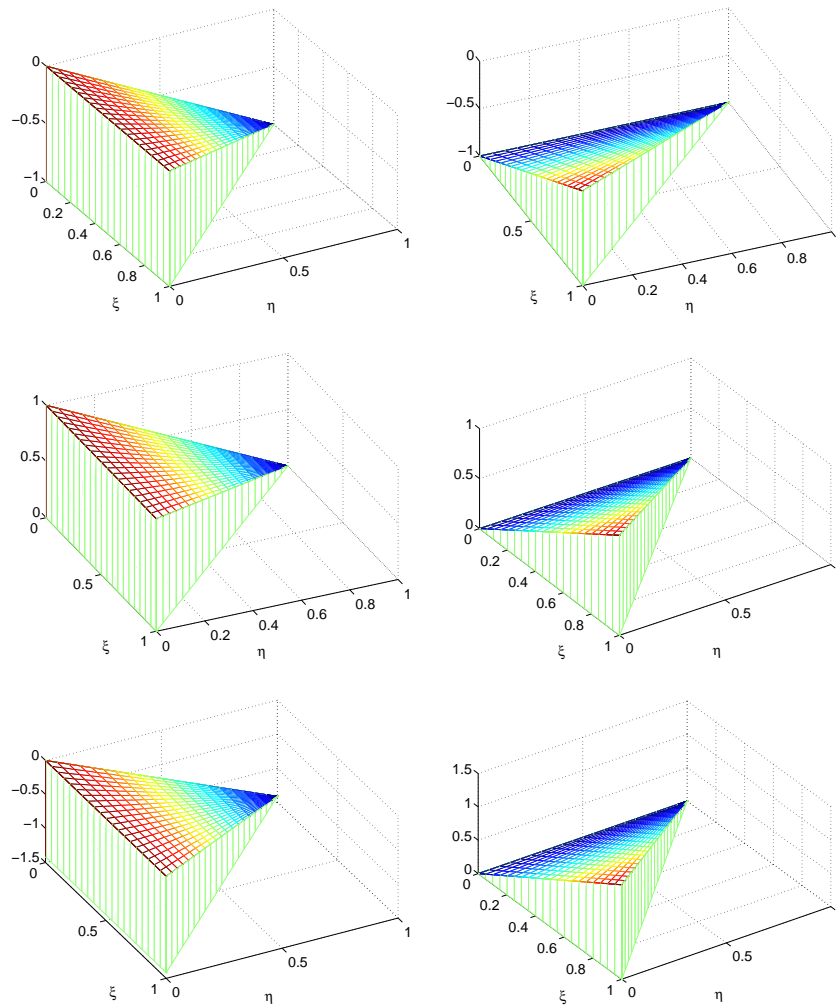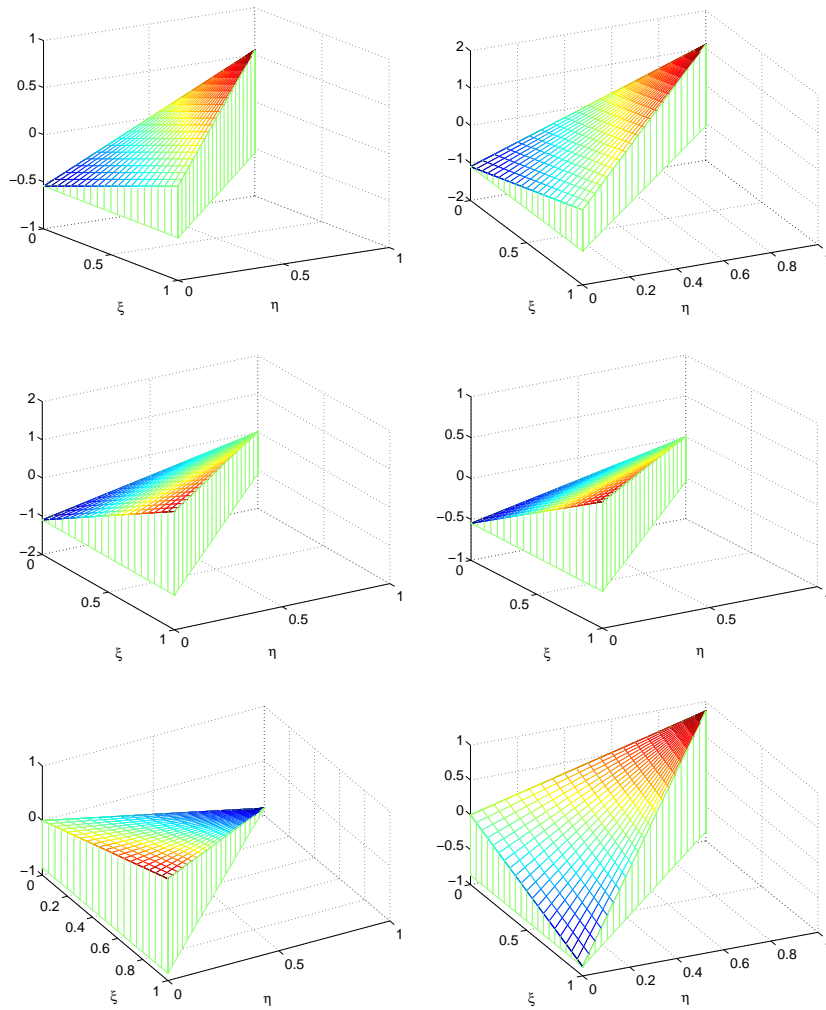
Figure 6: Shape functions of the zeroth order. Top left: $\Phi_{\Gamma_1}^{e,0}(1)$, top right: $\Phi_{\Gamma_1}^{e,0}(2)$; middle left: $\Phi_{\Gamma_2}^{e,0}(1)$, middle right: $\Phi_{\Gamma_2}^{e,0}(2)$; bottom left: $\Phi_{\Gamma_3}^{e,0}(1)$, bottom right: $\Phi_{\Gamma_3}^{e,0}(2)$.

$$\mathbf{\Phi}_{\Gamma_3}^{e,3} = \frac{\sqrt{7}}{4} \left[5(\eta-\xi)^3 - 3(\eta-\xi) \right] \begin{bmatrix} -1 \\ 1 \end{bmatrix},$$

$$\mathbf{\Phi}_{\Gamma_1}^{n,3} = 4\sqrt{105}\,\eta(1-\xi-\eta)(1-\xi-2\eta) \begin{bmatrix} 1 \\ 0 \end{bmatrix},$$

$$\mathbf{\Phi}_{\Gamma_2}^{n,3} = 4\sqrt{105}\,\xi(1-\xi-\eta)(2\xi+\eta-1) \begin{bmatrix} 0 \\ 1 \end{bmatrix},$$

$$\mathbf{\Phi}_{\Gamma_3}^{n,3} = -2\sqrt{210}\,\xi\eta(\eta-\xi) \begin{bmatrix} 1 \\ 1 \end{bmatrix},$$

$$\mathbf{\Phi}_{0,0}^{b,3} = 12\sqrt{35}\,\xi\eta(1-\xi-\eta) \otimes \left\{ \begin{bmatrix} 1 \\ 0 \end{bmatrix}, \begin{bmatrix} 0 \\ 1 \end{bmatrix} \right\}.$$

Figure 7: Shape functions of the first order. Top left: $\Phi^{e,1}_{\Gamma_1}(1)$, top right: $\Phi^{e,1}_{\Gamma_1}(2)$; middle left: $\Phi^{e,1}_{\Gamma_2}(1)$, middle right: $\Phi^{e,1}_{\Gamma_2}(2)$; bottom left: $\Phi^{e,1}_{\Gamma_3}(1)$, bottom right: $\Phi^{e,1}_{\Gamma_3}(2)$.

Fourth-order

$$\mathbf{\Phi}^{e,4}_{\Gamma_1} = -\frac{3\sqrt{10}}{80}[35(1-\xi-2\eta)^4-30(1-\xi-2\eta)^2+3]\begin{bmatrix} 1 \\ 2 \end{bmatrix},$$

$$\mathbf{\Phi}^{e,4}_{\Gamma_2} = \frac{3\sqrt{10}}{80}[35(2\xi+\eta-1)^4-30(2\xi+\eta-1)^2+3]\begin{bmatrix} 2 \\ 1 \end{bmatrix},$$

$$\mathbf{\Phi}^{e,4}_{\Gamma_3} = \frac{3}{16}[35(\eta-\xi)^4-30(\eta-\xi)^2+3]\begin{bmatrix} -1 \\ 1 \end{bmatrix},$$

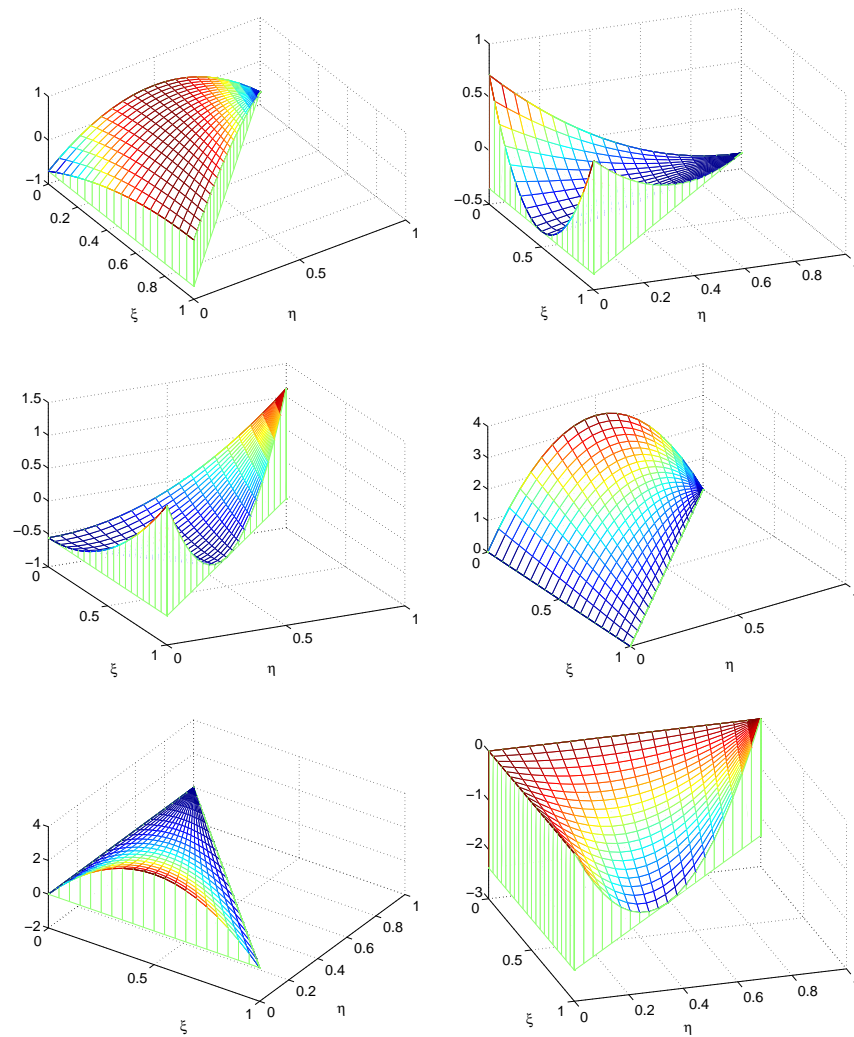$$\mathbf{\Phi}^{n,4}_{\Gamma_1} = 15\eta(1-\xi-\eta)[7(1-\xi-2\eta)^2-(1-\xi)^2]\begin{bmatrix} 1 \\ 0 \end{bmatrix},$$

Figure 8: Shape functions of the second order. Top left: $\Phi_{\Gamma_1}^{e,2}(1)$, with $\Phi_{\Gamma_1}^{e,2}(2)=2\Phi_{\Gamma_1}^{e,2}(1)$; top right: $\Phi_{\Gamma_1}^{e,2}(2)$, with $\Phi_{\Gamma_2}^{e,2}(1)=2\Phi_{\Gamma_2}^{e,2}(2)$; middle left: $\Phi_{\Gamma_3}^{e,2}(2)$, with $\Phi_{\Gamma_3}^{e,2}(1)=-\Phi_{\Gamma_3}^{e,2}(2)$; middle right: $\Phi_{\Gamma_1}^{n,2}(1)$, with $\Phi_{\Gamma_1}^{n,2}(2)=0$; bottom left: $\Phi_{\Gamma_2}^{n,2}(2)$, with $\Phi_{\Gamma_2}^{n,2}(1)=0$; bottom right: $\Phi_{\Gamma_3}^{n,2}(1)$, with $\Phi_{\Gamma_3}^{n,2}(2)=\Phi_{\Gamma_3}^{n,2}(1)$.

$$\mathbf{\Phi}_{\Gamma_2}^{n,4}=15\xi(1-\xi-\eta)[7(2\xi+\eta-1)^2-(1-\eta)^2]\begin{bmatrix} 0 \\ 1 \end{bmatrix},$$

$$\mathbf{\Phi}_{\Gamma_3}^{n,4}=-\frac{15\sqrt{2}}{2}\xi\eta[7(\eta-\xi)^2-(\xi+\eta)^2]\begin{bmatrix} 1 \\ 1 \end{bmatrix},$$

$$\mathbf{\Phi}_{1,0}^{b,4}=60\sqrt{21}\xi\eta(1-\xi-\eta)(2\eta+\xi-1)\otimes\left\{\begin{bmatrix} 1 \\ 0 \end{bmatrix},\begin{bmatrix} 0 \\ 1 \end{bmatrix}\right\},$$

$$\mathbf{\Phi}_{0,1}^{b,4}=60\sqrt{7}\xi\eta(1-\xi-\eta)(3\xi-1)\otimes\left\{\begin{bmatrix} 1 \\ 0 \end{bmatrix},\begin{bmatrix} 0 \\ 1 \end{bmatrix}\right\}.$$

Figure 9: Shape functions of the third order. Top left: $\Phi^{e,3}_{\Gamma_1}(1)$, with $\Phi^{e,3}_{\Gamma_1}(2) = 2\Phi^{e,3}_{\Gamma_1}(1)$; top right: $\Phi^{e,3}_{\Gamma_2}(2)$, with $\Phi^{e,3}_{\Gamma_2}(1) = 2\Phi^{e,3}_{\Gamma_2}(2)$; middle left: $\Phi^{e,3}_{\Gamma_3}(2)$, with $\Phi^{e,3}_{\Gamma_3}(1) = -\Phi^{e,3}_{\Gamma_3}(2)$; middle right: $\Phi^{n,3}_{\Gamma_1}(1)$, with $\Phi^{n,3}_{\Gamma_1}(2) = 0$; bottom left: $\Phi^{n,3}_{\Gamma_2}(2)$, with $\Phi^{n,3}_{\Gamma_2}(1) = 0$; bottom right: $\Phi^{n,3}_{\Gamma_3}(1)$, with $\Phi^{n,3}_{\Gamma_3}(2) = \Phi^{n,3}_{\Gamma_3}(1)$.

Figure 10: (Left) Shape functions of the third order. Shown is the graph for the function $C^{b,3}_{0,0}(\xi,\eta) = 12\sqrt{35}\xi\eta(1-\xi-\eta)$, with the bubble function $\Phi^{b,3}_{0,0}(\xi,\eta) = C^{b,3}_{0,0}(\xi,\eta) \otimes \bowtie$.
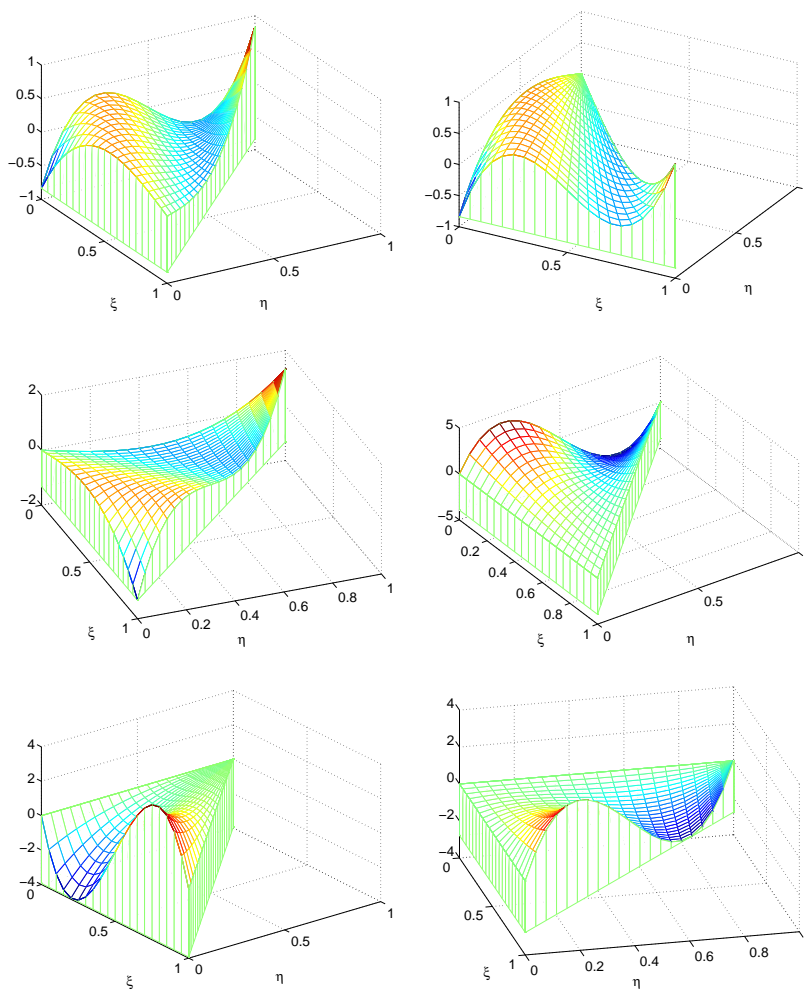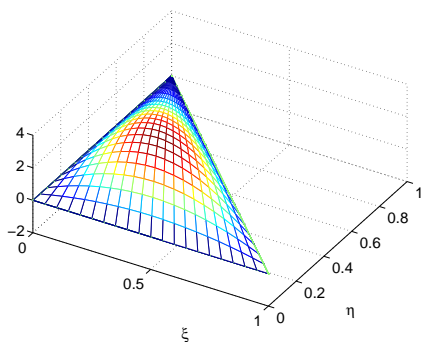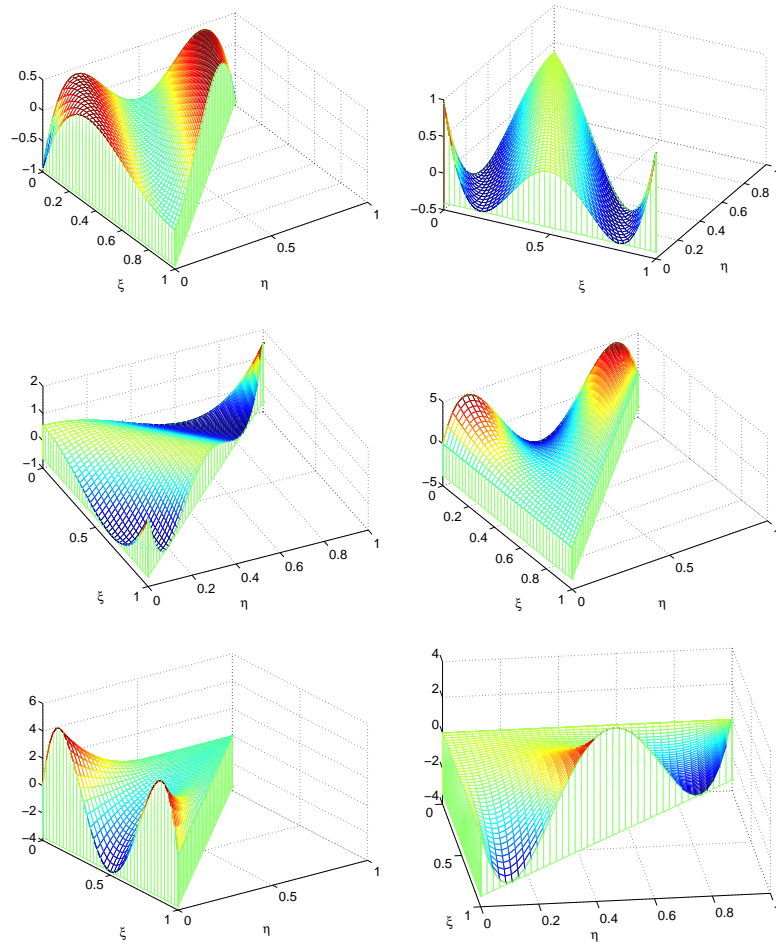
Figure 11: Shape functions of the fourth order. Top left: $\Phi_{\Gamma_1}^{e,4}(1)$, with $\Phi_{\Gamma_1}^{e,4}(2)=2\Phi_{\Gamma_1}^{e,4}(1)$; top right: $\Phi_{\Gamma_2}^{e,4}(2)$, with $\Phi_{\Gamma_2}^{e,4}(1)=2\Phi_{\Gamma_2}^{e,4}(2)$; middle left: $\Phi_{\Gamma_3}^{e,4}(2)$, with $\Phi_{\Gamma_3}^{e,4}(1)=-\Phi_{\Gamma_3}^{e,4}(2)$; middle right: $\Phi_{\Gamma_1}^{n,4}(1)$, with $\Phi_{\Gamma_1}^{n,4}(2)=0$; bottom left: $\Phi_{\Gamma_2}^{n,4}(2)$, with $\Phi_{\Gamma_2}^{n,4}(1)=0$; bottom right: $\Phi_{\Gamma_3}^{n,4}(1)$, with $\Phi_{\Gamma_3}^{n,4}(2)=\Phi_{\Gamma_3}^{n,4}(1)$.

Figure 12: Shape functions of the fourth order. Left: the graph for the function $C_{1,0}^{b,4}(\xi,\eta)=60\sqrt{21}\xi\eta(1-\xi-\eta)(2\eta+\xi-1)$, with the bubble function $\Phi_{1,0}^{b,4}(\xi,\eta)=C_{1,0}^{b,4}(\xi,\eta)\otimes\bowtie$; right: the graph for the function $C_{0,1}^{b,4}(\xi,\eta)=60\sqrt{7}\xi\eta(1-\xi-\eta)(3\xi-1)$, with the bubble function $\Phi_{0,1}^{b,4}(\xi,\eta)=C_{0,1}^{b,4}(\xi,\eta)\otimes\bowtie$.

Figure 13: Shape functions of the fifth order. Top left: $\Phi_{\Gamma_1}^{e,5}(1)$, with $\Phi_{\Gamma_1}^{e,5}(2) = 2\Phi_{\Gamma_1}^{e,5}(1)$; top right: $\Phi_{\Gamma_2}^{e,5}(2)$, with $\Phi_{\Gamma_2}^{e,5}(1) = 2\Phi_{\Gamma_2}^{e,5}(2)$; middle left: $\Phi_{\Gamma_3}^{e,5}(2)$, with $\Phi_{\Gamma_3}^{e,5}(1) = -\Phi_{\Gamma_3}^{e,5}(2)$; middle right: $\Phi_{\Gamma_1}^{n,5}(1)$, with $\Phi_{\Gamma_1}^{n,5}(2) = 0$; bottom left: $\Phi_{\Gamma_2}^{n,5}(2)$, with $\Phi_{\Gamma_2}^{n,5}(1) = 0$; bottom right: $\Phi_{\Gamma_3}^{n,5}(1)$, with $\Phi_{\Gamma_3}^{n,5}(2) = \Phi_{\Gamma_3}^{n,5}(1)$.
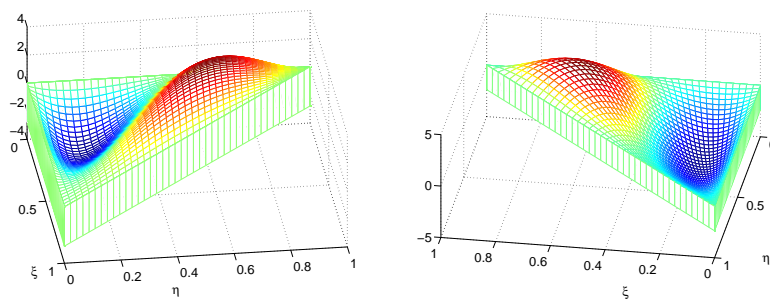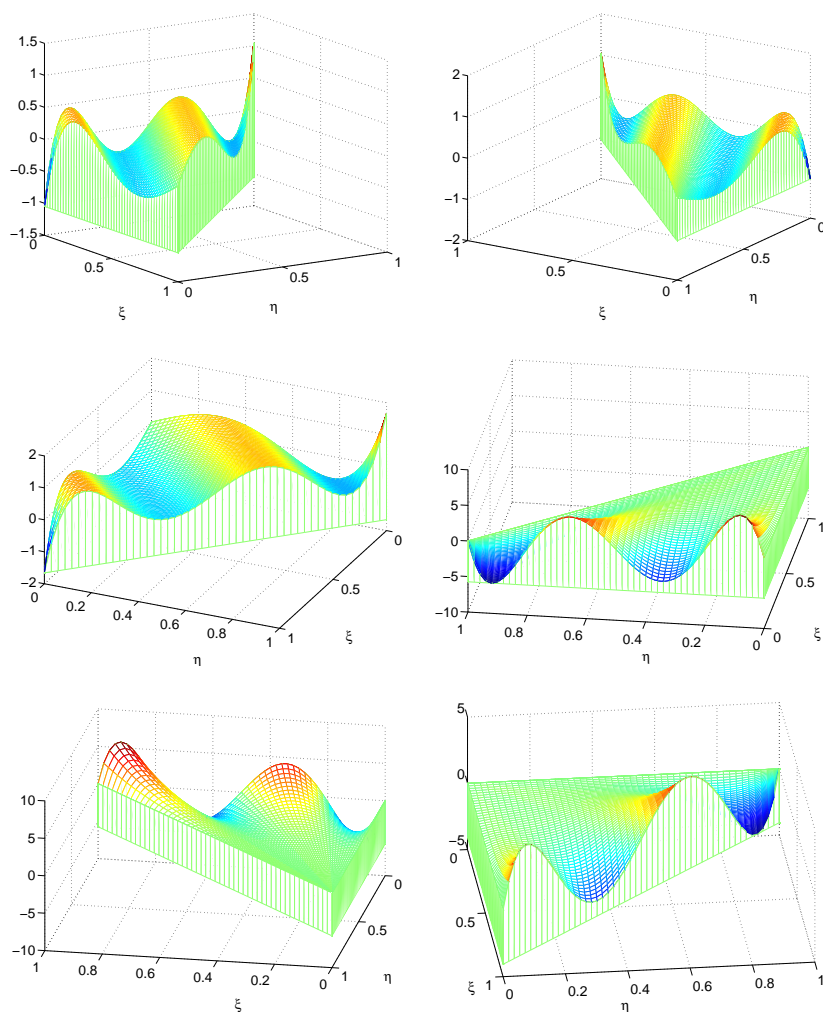
Fifth-order

$$\boldsymbol{\Phi}_{\Gamma_1}^{e,5} = -\frac{\sqrt{110}}{80}[63(1-\xi-2\eta)^5 - 70(1-\xi-2\eta)^3 + 15(1-\xi-2\eta)]\begin{bmatrix} 1 \\ 2 \end{bmatrix},$$

$$\boldsymbol{\Phi}_{\Gamma_2}^{e,5} = \frac{\sqrt{110}}{80}[63(2\xi+\eta-1)^5 - 70(2\xi+\eta-1)^3 + 15(2\xi+\eta-1)]\begin{bmatrix} 2 \\ 1 \end{bmatrix},$$

$$\boldsymbol{\Phi}_{\Gamma_3}^{e,5} = \frac{\sqrt{11}}{16}[63(\eta-\xi)^5 - 70(\eta-\xi)^3 + 15(\eta-\xi)]\begin{bmatrix} -1 \\ 1 \end{bmatrix},$$
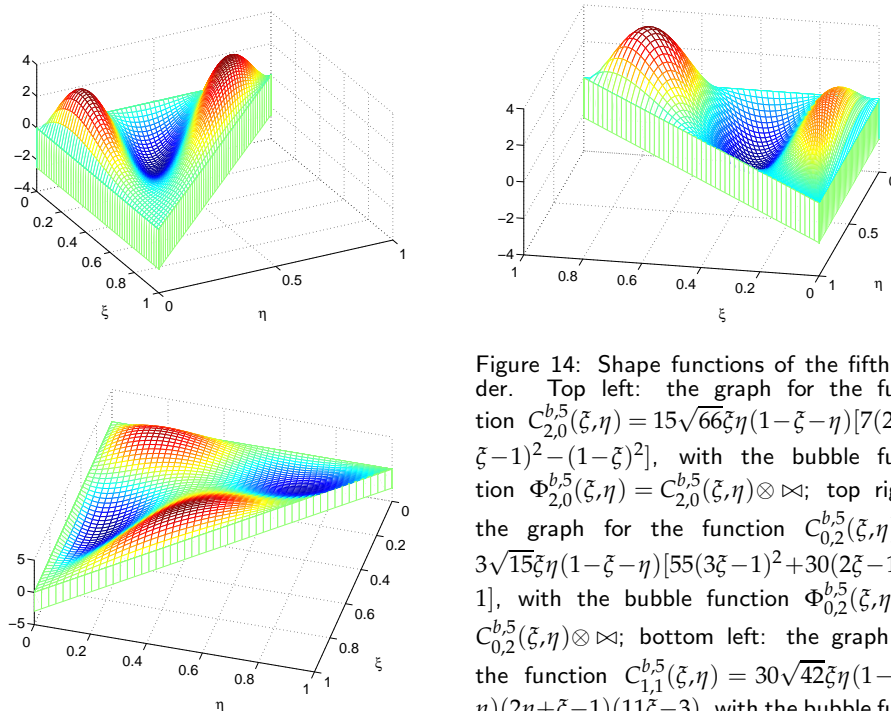
Figure 14: Shape functions of the fifth order. Top left: the graph for the function $C_{2,0}^{b,5}(\xi,\eta) = 15\sqrt{66}\xi\eta(1-\xi-\eta)[7(2\eta+\xi-1)^2-(1-\xi)^2]$, with the bubble function $\Phi_{2,0}^{b,5}(\xi,\eta) = C_{2,0}^{b,5}(\xi,\eta)\otimes\bowtie$; top right: the graph for the function $C_{0,2}^{b,5}(\xi,\eta) = 3\sqrt{15}\xi\eta(1-\xi-\eta)[55(3\xi-1)^2+30(2\xi-1)-1]$, with the bubble function $\Phi_{0,2}^{b,5}(\xi,\eta) = C_{0,2}^{b,5}(\xi,\eta)\otimes\bowtie$; bottom left: the graph for the function $C_{1,1}^{b,5}(\xi,\eta) = 30\sqrt{42}\xi\eta(1-\xi-\eta)(2\eta+\xi-1)(11\xi-3)$, with the bubble function $\Phi_{1,1}^{b,5}(\xi,\eta) = C_{1,1}^{b,5}(\xi,\eta)\otimes\bowtie$.

$$\mathbf{\Phi}_{\Gamma_1}^{n,5} = 3\sqrt{770}\eta(1-\xi-\eta)(1-\xi-2\eta)[3(1-\xi-2\eta)^2-(1-\xi)^2]\begin{bmatrix}1\\0\end{bmatrix},$$

$$\mathbf{\Phi}_{\Gamma_2}^{n,5} = 3\sqrt{770}\xi(1-\xi-\eta)(2\xi+\eta-1)[3(2\xi+\eta-1)^2-(1-\eta)^2]\begin{bmatrix}0\\1\end{bmatrix},$$

$$\mathbf{\Phi}_{\Gamma_3}^{n,5} = -3\sqrt{385}\xi\eta(\eta-\xi)[3(\eta-\xi)^2-(\xi+\eta)^2]\begin{bmatrix}1\\1\end{bmatrix},$$

$$\mathbf{\Phi}_{2,0}^{b,5} = 15\sqrt{66}\xi\eta(1-\xi-\eta)[7(2\eta+\xi-1)^2-(1-\xi)^2]\otimes\left\{\begin{bmatrix}1\\0\end{bmatrix},\begin{bmatrix}0\\1\end{bmatrix}\right\},$$

$$\mathbf{\Phi}_{0,2}^{b,5} = 3\sqrt{15}\xi\eta(1-\xi-\eta)[55(2\xi-1)^2+30(2\xi-1)-1]\otimes\left\{\begin{bmatrix}1\\0\end{bmatrix},\begin{bmatrix}0\\1\end{bmatrix}\right\},$$

$$\mathbf{\Phi}_{1,1}^{b,5} = 30\sqrt{42}\xi\eta(1-\xi-\eta)(2\eta+\xi-1)(11\xi-3)\otimes\left\{\begin{bmatrix}1\\0\end{bmatrix},\begin{bmatrix}0\\1\end{bmatrix}\right\}.$$

Sixth-order

$$\mathbf{\Phi}_{\Gamma_1}^{e,6} = -\frac{\sqrt{130}}{160}[231(1-\xi-2\eta)^6-315(1-\xi-2\eta)^4+105(1-\xi-2\eta)^2-5]\begin{bmatrix}1\\2\end{bmatrix},$$

$$\mathbf{\Phi}_{\Gamma_2}^{e,6} = \frac{\sqrt{130}}{160}[231(2\xi+\eta-1)^6-315(2\xi+\eta-1)^4+105(2\xi+\eta-1)^2-5]\begin{bmatrix}2\\1\end{bmatrix},$$

$$\Phi_{\Gamma_3}^{e,6} = \frac{\sqrt{13}}{32}[231(\eta-\xi)^6 - 315(\eta-\xi)^4 + 105(\eta-\xi)^2 - 5]\begin{bmatrix} -1 \\ 1 \end{bmatrix},$$

$$\Phi_{\Gamma_1}^{n,6} = \frac{7}{8}\sqrt{390}\eta(1-\xi-\eta)[33(1-\xi-2\eta)^4 - 18(1-\xi-2\eta)^2(1-\xi)^2 + (1-\xi)^4]\begin{bmatrix} 1 \\ 0 \end{bmatrix},$$

$$\Phi_{\Gamma_2}^{n,6} = \frac{7}{8}\sqrt{390}\xi(1-\xi-\eta)[33(2\xi+\eta-1)^4 - 18(2\xi+\eta-1)^2(1-\eta)^2 + (1-\eta)^4]\begin{bmatrix} 0 \\ 1 \end{bmatrix},$$

$$\Phi_{\Gamma_3}^{n,6} = -\frac{7}{8}\sqrt{195}\xi\eta[33(\eta-\xi)^4 - 18(\eta-\xi)^2(\xi+\eta)^2 + (\xi+\eta)^4]\begin{bmatrix} 1 \\ 1 \end{bmatrix},$$

$$\Phi_{3,0}^{b,6} = 21\sqrt{1430}\xi\eta(1-\xi-\eta)[3(2\eta+\xi-1)^3 - (2\eta+\xi-1)(1-\xi)^2] \otimes \left\{ \begin{bmatrix} 1 \\ 0 \end{bmatrix}, \begin{bmatrix} 0 \\ 1 \end{bmatrix} \right\},$$

$$\Phi_{0,3}^{b,6} = \frac{3}{4}\sqrt{210}\xi\eta(1-\xi-\eta)[143(2\xi-1)^3 + 99(2\xi-1)^2 - 11(2\xi-1) - 7] \otimes \left\{ \begin{bmatrix} 1 \\ 0 \end{bmatrix}, \begin{bmatrix} 0 \\ 1 \end{bmatrix} \right\},$$

$$\Phi_{2,1}^{b,6} = \frac{3}{2}\sqrt{770}\xi\eta(1-\xi-\eta)[7(2\eta+\xi-1)^2 - (1-\xi)^2][7+13(2\xi-1)] \otimes \left\{ \begin{bmatrix} 1 \\ 0 \end{bmatrix}, \begin{bmatrix} 0 \\ 1 \end{bmatrix} \right\},$$

$$\Phi_{1,2}^{b,6} = \frac{105}{2}\sqrt{22}\xi\eta(1-\xi-\eta)(2\eta+\xi-1)[1+10(2\xi-1)+13(2\xi-1)^2] \otimes \left\{ \begin{bmatrix} 1 \\ 0 \end{bmatrix}, \begin{bmatrix} 0 \\ 1 \end{bmatrix} \right\}.$$

Seventh-order

$$\Phi_{\Gamma_1}^{e,7} = -\frac{\sqrt{6}}{32}[429(\star)^7 - 693(\star)^5 + 315(\star)^3 - 35(\star)]\begin{bmatrix} 1 \\ 2 \end{bmatrix},$$

$$\Phi_{\Gamma_2}^{e,7} = \frac{\sqrt{6}}{32}[429(*)^7 - 693(*)^5 + 315(*)^3 - 35(*)]\begin{bmatrix} 2 \\ 1 \end{bmatrix},$$

$$\Phi_{\Gamma_3}^{e,7} = \frac{\sqrt{15}}{32}[429(\eta-\xi)^7 - 693(\eta-\xi)^5 + 315(\eta-\xi)^3 - 35(\eta-\xi)]\begin{bmatrix} -1 \\ 1 \end{bmatrix},$$

$$\Phi_{\Gamma_1}^{n,7} = \frac{3}{14}\sqrt{35}\eta(1-\xi-\eta)[1001(\star)^5 - 770(\star)^3(1-\xi)^2 + 105(\star)(1-\xi)^4]\begin{bmatrix} 1 \\ 0 \end{bmatrix},$$

$$\Phi_{\Gamma_2}^{n,7} = \frac{3}{14}\sqrt{35}\xi(1-\xi-\eta)[1001(*)^5 - 770(*)^3(1-\eta)^2 + 105(*)(1-\eta)^4]\begin{bmatrix} 0 \\ 1 \end{bmatrix},$$

$$\Phi_{\Gamma_3}^{n,7} = -\frac{3}{28}\sqrt{70}\xi\eta[1001(\eta-\xi)^5 - 770(\eta-\xi)^3(\xi+\eta)^2 + 105(\eta-\xi)(\xi+\eta)^4]\begin{bmatrix} 1 \\ 1 \end{bmatrix},$$

$$\Phi_{4,0}^{b,7} = \frac{105}{2}\sqrt{13}\xi\eta(1-\xi-\eta)[33(\star)^4 - 18(\star)^2(1-\xi)^2 + (1-\xi)^4] \otimes \left\{ \begin{bmatrix} 1 \\ 0 \end{bmatrix}, \begin{bmatrix} 0 \\ 1 \end{bmatrix} \right\},$$

$$\Phi_{0,4}^{b,7} = \frac{1}{4}\sqrt{110}\xi\eta(1-\xi-\eta)[1365(\diamond)^4 + 1092(\diamond)^3 - 234(\diamond)^2 - 204(\diamond) - 3] \otimes \left\{ \begin{bmatrix} 1 \\ 0 \end{bmatrix}, \begin{bmatrix} 0 \\ 1 \end{bmatrix} \right\},$$

$$\Phi_{3,1}^{b,7} = 21\sqrt{1430}\xi\eta(1-\xi-\eta)[-3(\star)^3 + (\star)(1-\xi)^2][3+5(\diamond)] \otimes \left\{ \begin{bmatrix} 1 \\ 0 \end{bmatrix}, \begin{bmatrix} 0 \\ 1 \end{bmatrix} \right\},$$

$$\Phi_{1,3}^{b,7} = -\frac{3}{2}\sqrt{154}\xi\eta(1-\xi-\eta)(\star)[-15+65(\diamond)+455(\diamond)^2+455(\diamond)^3] \otimes \left\{ \begin{bmatrix} 1 \\ 0 \end{bmatrix}, \begin{bmatrix} 0 \\ 1 \end{bmatrix} \right\},$$

$$\Phi_{2,2}^{b,7} = \frac{3}{2}\sqrt{130}\xi\eta(1-\xi-\eta)[7(\star)^2 - (1-\xi)^2][17+98(\diamond)+105(\diamond)^2] \otimes \left\{ \begin{bmatrix} 1 \\ 0 \end{bmatrix}, \begin{bmatrix} 0 \\ 1 \end{bmatrix} \right\}.$$

Eighth-order

$$\mathbf{\Phi}_{\Gamma_1}^{e,8} = -\frac{\sqrt{170}}{1280}[6435(\star)^8 - 12012(\star)^6 + 6930(\star)^4 - 1260(\star)^2 + 35] \begin{bmatrix} 1 \\ 2 \end{bmatrix},$$

$$\mathbf{\Phi}_{\Gamma_2}^{e,8} = \frac{\sqrt{170}}{1280}[6435(*)^8 - 12012(*)^6 + 6930(*)^4 - 1260(*)^2 + 35] \begin{bmatrix} 2 \\ 1 \end{bmatrix},$$

$$\mathbf{\Phi}_{\Gamma_3}^{e,8} = \frac{\sqrt{17}}{256}[6435(\eta-\xi)^8 - 12012(\eta-\xi)^6 + 6930(\eta-\xi)^4 - 1260(\eta-\xi)^2 + 35] \begin{bmatrix} -1 \\ 1 \end{bmatrix},$$

$$\mathbf{\Phi}_{\Gamma_1}^{n,8} = \frac{9}{112}\sqrt{1190}\eta(\wr)[1001(\star)^6 - 1001(\star)^4(1-\xi)^2 + 231(\star)^2(1-\xi)^4 - 7(1-\xi)^6] \begin{bmatrix} 1 \\ 0 \end{bmatrix},$$

$$\mathbf{\Phi}_{\Gamma_2}^{n,8} = \frac{9}{112}\sqrt{1190}\xi(\wr)[1001(*)^6 - 1001(*)^4(1-\eta)^2 + 231(*)^2(1-\eta)^4 - 7(1-\eta)^6] \begin{bmatrix} 0 \\ 1 \end{bmatrix},$$

$$\mathbf{\Phi}_{\Gamma_3}^{n,8} = -\frac{9}{112}\sqrt{595}\xi\eta[1001(\dagger)^6 - 1001(\dagger)^4(\xi+\eta)^2 + 231(\dagger)^2(\xi+\eta)^4 - 7(\xi+\eta)^6] \begin{bmatrix} 1 \\ 1 \end{bmatrix},$$

$$\mathbf{\Phi}_{5,0}^{b,8} = \frac{9}{14}\sqrt{595}\xi\eta(\wr)[-1001(\star)^5 + 770(\star)^3(1-\xi)^2 - 105(\star)(1-\xi)^4] \otimes \left\{ \begin{bmatrix} 1 \\ 0 \end{bmatrix}, \begin{bmatrix} 0 \\ 1 \end{bmatrix} \right\},$$

$$\mathbf{\Phi}_{0,5}^{b,8} = \frac{3}{4}\sqrt{2310}\xi\eta(1-\xi-\eta)[221(\diamond)^5 + 195(\diamond)^4 - 65(\diamond)^3 - 65(\diamond)^2 + 2] \otimes \left\{ \begin{bmatrix} 1 \\ 0 \end{bmatrix}, \begin{bmatrix} 0 \\ 1 \end{bmatrix} \right\},$$

$$\mathbf{\Phi}_{4,1}^{b,8} = \frac{15}{4}\sqrt{273}\xi\eta(\wr)[33(\star)^4 - 18(\star)^2(1-\xi)^2 + (1-\xi)^4][11 + 17(\diamond)] \otimes \left\{ \begin{bmatrix} 1 \\ 0 \end{bmatrix}, \begin{bmatrix} 0 \\ 1 \end{bmatrix} \right\},$$

$$\mathbf{\Phi}_{1,4}^{b,8} = -\frac{15}{2}\sqrt{546}\xi\eta(\wr)(\star)[-2 - 14(\diamond) + 21(\diamond)^2 + 140(\diamond)^3 + 119(\diamond)^4] \otimes \left\{ \begin{bmatrix} 1 \\ 0 \end{bmatrix}, \begin{bmatrix} 0 \\ 1 \end{bmatrix} \right\},$$

$$\mathbf{\Phi}_{3,2}^{b,8} = 105\sqrt{66}\xi\eta(1-\xi-\eta)[-3(\star)^3 + (\star)(1-\xi)^2][4 + 18(\diamond) + 17(\diamond)^2] \otimes \left\{ \begin{bmatrix} 1 \\ 0 \end{bmatrix}, \begin{bmatrix} 0 \\ 1 \end{bmatrix} \right\},$$

$$\mathbf{\Phi}_{2,3}^{b,8} = \frac{45}{2}\sqrt{182}\xi\eta(1-\xi-\eta)[7(\star)^2 - (1-\xi)^2][6(\diamond) + 21(\diamond)^2 + 17(\diamond)^3] \otimes \left\{ \begin{bmatrix} 1 \\ 0 \end{bmatrix}, \begin{bmatrix} 0 \\ 1 \end{bmatrix} \right\}.$$

Ninth-order

$$\mathbf{\Phi}_{\Gamma_1}^{e,9} = -\frac{\sqrt{190}}{1280}[12155(\star)^9 - 25740(\star)^7 + 18018(\star)^5 - 4620(\star)^3 + 315(\star)] \begin{bmatrix} 1 \\ 2 \end{bmatrix},$$

$$\mathbf{\Phi}_{\Gamma_2}^{e,9} = \frac{\sqrt{190}}{1280}[12155(*)^9 - 25740(*)^7 + 18018(*)^5 - 4620(*)^3 + 315(*)] \begin{bmatrix} 2 \\ 1 \end{bmatrix},$$

$$\mathbf{\Phi}_{\Gamma_3}^{e,9} = \frac{\sqrt{19}}{256}[12155(\dagger)^9 - 25740(\dagger)^7 + 18018(\dagger)^5 - 4620(\dagger)^3 + 315(\dagger)] \begin{bmatrix} -1 \\ 1 \end{bmatrix},$$

$$\mathbf{\Phi}_{\Gamma_1}^{n,9} = \frac{15}{8}\sqrt{209}\eta(\wr)[221(\star)^7 - 273(\star)^5(1-\xi)^2 + 91(\star)^3(1-\xi)^4 - 7(\star)(1-\xi)^6] \begin{bmatrix} 1 \\ 0 \end{bmatrix},$$

$$\mathbf{\Phi}_{\Gamma_2}^{n,9} = \frac{15}{8}\sqrt{209}\xi(\wr)[221(*)^7 - 273(*)^5(1-\eta)^2 + 91(*)^3(1-\eta)^4 - 7(*)(1-\eta)^6] \begin{bmatrix} 0 \\ 1 \end{bmatrix},$$

$$\mathbf{\Phi}_{\Gamma_3}^{n,9} = -\frac{15}{16}\sqrt{418}\xi\eta[221(\dagger)^7 - 273(\dagger)^5(\xi+\eta)^2 + 91(\dagger)^3(\xi+\eta)^4 - 7(\dagger)(\xi+\eta)^6] \begin{bmatrix} 1 \\ 1 \end{bmatrix},$$

$$\Phi_{6,0}^{b,9}=\frac{45}{56}\sqrt{2261}\xi\eta(\wr)[1001(\star)^6-1001(\star)^4(1-\xi)^2+231(\star)^2(1-\xi)^4-7(1-\xi)^6]\otimes\bowtie,$$

$$\Phi_{0,6}^{b,9}=\frac{15}{56}\sqrt{91}\xi\eta(\wr)[6783(\diamond)^6+6426(\diamond)^5-2975(\diamond)^4-3320(\diamond)^3+105(\diamond)^2+266(\diamond)+7]\otimes\bowtie,$$

$$\Phi_{5,1}^{b,9}=\frac{15}{56}\sqrt{357}\xi\eta(\wr)[-1001(\star)^5+770(\star)^3(1-\xi)^2-105(\star)(1-\xi)^4][13+19(\diamond)]\otimes\bowtie,$$

$$\Phi_{1,5}^{b,9}=-\frac{5}{4}\sqrt{182}\xi\eta(\wr)(\star)[9-165(\diamond)-750(\diamond)^2+510(\diamond)^3+3825(\diamond)^4+2907(\diamond)^5]\otimes\bowtie,$$

$$\Phi_{4,2}^{b,9}=\frac{5}{8}\sqrt{1547}\xi\eta(\wr)[33(\star)^4-18(\star)^2(1-\xi)^2+(1-\xi)^4][51+198(\diamond)+171(\diamond)^2]\otimes\bowtie,$$

$$\Phi_{2,4}^{b,9}=\frac{15}{4}\sqrt{14}\xi\eta(\wr)[7(\star)^2-(1-\xi)^2][-19-28(\diamond)+510(\diamond)^2+1428(\diamond)^3+969(\diamond)^4]\otimes\bowtie,$$

$$\Phi_{3,3}^{b,9}=\frac{15}{4}\sqrt{154}\xi\eta(\wr)[-3(\star)^3+(\star)(1-\xi)^2][39+527(\diamond)+1377(\diamond)^2+969(\diamond)^3]\otimes\bowtie.$$

Tenth-order

$$\Phi_{\Gamma_1}^{e,10}=-\frac{\sqrt{210}}{2560}[46189(\star)^{10}-109395(\star)^8+90090(\star)^6-30030(\star)^4+3465(\star)^2-63]\begin{bmatrix}1\\2\end{bmatrix},$$

$$\Phi_{\Gamma_2}^{e,10}=\frac{\sqrt{210}}{2560}[46189(*)^{10}-109395(*)^8+90090(*)^6-30030(*)^4+3465(*)^2-63]\begin{bmatrix}2\\1\end{bmatrix},$$

$$\Phi_{\Gamma_3}^{e,10}=\frac{\sqrt{21}}{512}[46189(\dagger)^{10}-109395(\dagger)^8+90090(\dagger)^6-30030(\dagger)^4+3465(\dagger)^2-63]\begin{bmatrix}-1\\1\end{bmatrix},$$

$$\Phi_{\Gamma_1}^{n,10}=\frac{11}{320}\sqrt{35}\eta(\wr)[62985\star^8-92820\star^6\natural^2+40950\star^4\natural^4-5460\star^2\natural^6+105\natural^8]\begin{bmatrix}1\\0\end{bmatrix},$$

$$\Phi_{\Gamma_2}^{n,10}=\frac{11}{320}\sqrt{35}\xi(\wr)[62985*^8-92820*^6\sharp^2+40950*^4\sharp^4-5460*^2\sharp^6+105\sharp^8]\begin{bmatrix}0\\1\end{bmatrix},$$

$$\Phi_{\Gamma_3}^{n,10}=-\frac{11}{640}\sqrt{70}\xi\eta[62985\dagger^8-92820\dagger^6\flat^2+40950\dagger^4\flat^4-5460\dagger^2\flat^6+105\flat^8]\begin{bmatrix}1\\1\end{bmatrix},$$

$$\Phi_{7,0}^{b,10}=\frac{165}{8}\sqrt{399}\xi\eta(\wr)[-221(\star)^7+273(\star)^5(1-\xi)^2-91(\star)^3(1-\xi)^4+7(\star)(1-\xi)^6]\otimes\bowtie,$$

$$\Phi_{0,7}^{b,10}=\frac{1}{48}\sqrt{15015}\xi\eta(\wr)[14535(\diamond^7+\diamond^6)-8721\diamond^5-9945\diamond^4+765\diamond^3+1485\diamond^2+45\diamond-27]\otimes\bowtie,$$

$$\Phi_{6,1}^{b,10}=\frac{15}{112}\sqrt{74613}\xi\eta(\wr)[1001\star^6-1001\star^4\natural^2+231\star^2\natural^4-7\natural^6][5+7(\diamond)]\otimes\bowtie,$$

$$\Phi_{1,6}^{b,10}=-\frac{15}{8}\sqrt{77}\xi\eta(\wr)(\star)[23+122\diamond-799\diamond^2-3060\diamond^3+969\diamond^4+9690\diamond^5+6783\diamond^6]\otimes\bowtie,$$

$$\Phi_{5,2}^{b,10}=\frac{3}{112}\sqrt{21945}\xi\eta(\wr)[-1001\star^5+770\star^3\natural^2-105\star\natural^4][37+130\diamond+105\diamond^2]\otimes\bowtie,$$

$$\Phi_{2,5}^{b,10}=\frac{15}{112}\sqrt{154}\xi\eta(\wr)[7\star^2-\natural^2][-77-1547\diamond-2142\diamond^2+13566\diamond^3+33915\diamond^4+20349\diamond^5]\otimes\bowtie,$$

$$\Phi_{4,3}^{b,10}=\frac{3}{32}\sqrt{51051}\xi\eta(\wr)[33\star^4-18\star^2\natural^2+\natural^4][55+475\diamond+1045\diamond^2+665\diamond^3]\otimes\bowtie,$$

$$\Phi_{3,4}^{b,10}=\frac{11}{8}\sqrt{238}\xi\eta(\wr)[-3\star^3+\star\natural^2][-75+540\diamond+5130\diamond^2+10260\diamond^3+5985\diamond^4]\otimes\bowtie.$$

Symbols in formulas above are defined at the beginning of the Appendix.

References

[1] R. Abdul-Rahman and M. Kasper, Orthogonal hierarchical Nédélec elements, IEEE Trans. Magn., 44 (2008), 1210–1213.

[2] S. Adjerid, M. Aiffa and J. E. Flaherty, Hierarchical finite element bases for triangular and tetrahedral elements, Comput. Methods. Appl. Mech. Engrg., 190 (2001), 2925–2941.

[3] M. Ainsworth and J. Coyle, Hierarchic hp-edge element families for Maxwell's equations on hybrid quadrilateral/triangular meshes, Comput. Methods. Appl. Mech. Engrg., 190 (2001), 6709–6733.

[4] M. Ainsworth and J. Coyle, Conditioning of hierarchic p-version Nédélec elements on meshes of curvilinear quadrilaterals and hexahedra, SIAM J. Numer. Anal., 41 (2003), 731–750.

[5] M. Ainsworth and J. Coyle, Hierarchic finite element bases on unstructured tetrahedral meshes, Int. J. Numer. Methods. Engrg., 58 (2003), 2103–2130.

[6] I. Babuška, B. A. Szabo and I. N. Katz, The p-version of the finite element method, SIAM J. Numer. Anal., 18 (1981), 515–545.

[7] M. L. Bittencourt, Fully tensorial nodal and modal shape functions for triangles and tetrahedra, Int. J. Numer. Methods. Engrg., 63 (2005), 1530–1558.

[8] A. Bossavit, Computational Electromagnetism, Academic Press, New York, 1998.

[9] C. F. Dunkl and Y. Xu, Orthogonal Polynomials of Several Variables, Encyclopedia of Mathematics and Its Applications, 81, Cambridge University Press, Cambridge, 2001.

[10] F. Zhang (Editor), The Schur Complement and Its Applications, Springer-Verlag, New York, 2005.

[11] J. Gopalakrishnan, L. E. García-Castillo and L. F. Demkowicz, Nédélec spaces in affine coordinates, Comput. Math. Appl., 49 (2005), 1285–1294.

[12] R. Hiptmair, Canonical construction of finite elements, Math. Comput., 68 (1999), 1325–1346.

[13] R. Hiptmair, Higher order Whitney forms, PIER., 32 (2001), 271–299.

[14] P. Ingelström, A new set of H (curl)-conforming hierarchical basis functions for tetrahedral meshes, IEEE Trans. Microw. Theor. Tech., 54 (2006), 106–114.

[15] E. Jørgensen, J. L. Volakis, P. M. Meincke and O. Breinbjerg, Higher order hierarchical Legendre basis functions for electromagnetic modeling, IEEE Trans. Antenna. Propaga., 52 (2004), 2985–2995.

[16] G. E. Karniadakis and S. J. Sherwin, Spectral/hp Element Methods for CFD, Oxford University Press, New York, 1999.

[17] J. C. Nédélec, Mixed finite elements in $\mathbb{R}^3$, Numer. Math., 35 (1980), 315–341.

[18] W. Rachowicz and L. Demkowicz, An hp-adaptive finite element method for electromagnetics, II, a 3D implementation, Int. J. Numer. Methods. Engrg., 53 (2002), 147–180.

[19] F. Rapetti, High order edge elements on simplicial meshes, ESAIM: M2AN, 41 (2007), 1001–1020.

[20] F. Rapetti and A. Bossavit, Whitney forms of higher degree, SIAM J. Numer. Anal., 47 (2009), 2369–2386.

[21] Z. Ren and N. Ida, High order differential form-based elements for the computation of electromagnetic field, IEEE Trans. Magn., 36 (2000), 1472–1478.

[22] J. Schöberl and S. Zaglmayr, High order Nédélec elements with local complete sequence properties, Compel., 24 (2005), 374–384.

[23] J. Shen, Efficient spectral-Galerkin method, I, direct solvers of second- and fourth-order equations using Legendre polynomials, SIAM J. Sci. Comput., 15 (1994), 1489–1505.

[24] I. A. Shreshevskii, Orthogonalization of graded sets of vectors, J. Nonlinear. Math. Phys., 8 (2001), 54–58.

[25] D.-K. Sun, J.-F. Lee and Z. Cendes, Construction of nearly orthogonal Nedelec bases for rapid convergence with multilevel preconditioned solvers, SIAM J. Sci. Comput., 23 (2001), 1053–1076.

[26] B. Szabó and I. Babuška, Finite Element Analysis, John Wiley & Sons, New York, 1991.

[27] J. P. Webb, Hierarchal vector basis functions of arbitrary order for triangular and tetrahedral finite elements, IEEE Trans. Antenna. Propaga., 47 (1999), 1244–1253.

[28] H. Whitney, Geometric Integration Theory, Princeton University Press, Princeton, 1957.

[29] J. Xin, K. Pinchedez and J. E. Flaherty, Implementation of hierarchical bases in FEMLAB for simplicial elements, ACM Trans. Math. Software., 31 (2005), 187–200.